Jurnal Fisika Flux: Jurnal Ilmiah Fisika FMIPA Universitas Lambung Mangkurat
Volume 23, Nomor 1, Februari 2026
1819-796X (p-ISSN); 2541-1713 (e-ISSN)
https://ppjp.ulm.ac.id/journal/index.php/f *Research Article*

Spatial Dynamics of Mangrove Forests in Kuala Lupak Nature Reserve: A Google Earth Engine-Based Analysis using NDVI and MVI

Widya Edma Putri, Nurlina*, Sri Cahyo Wahyono, Ichsan Ridwan
Physics Department, Faculty of Mathematics dan Natural Sciences, Lambung Mangkurat University

*Email korespondensi : nurlina_abdullah@ulm.ac.id

DOI: https://doi.org//10.20527/flux.v23i1.2470

Submitted: 08 December 2025; Revised: 07 May 2026; Accepted: 10 May 2026

ABSTRACT

This study aims to analyze the dynamics of mangrove cover in the Kuala Lupak Nature Reserve, South Kalimantan, using multitemporal Landsat imagery and Random Forest classification on Google Earth Engine. Two vegetation indices, Normalized Difference Vegetation Index (NDVI) and Mangrove Vegetation Index (MVI), were applied to improve mangrove discrimination across observation years (1990, 2000, 2010, and 2020). The results indicate that MVI tends to provide more stable classification performance compared to NDVI, with overall accuracy values generally exceeding 0,90. The analysis of mangrove change shows a decreasing trend over the 30-year period, with a total loss of 1,857.15 ha and a gain of 318.15 ha, resulting in a net loss of approximately 1,539 ha. However, these results are derived from classified satellite data and may be influenced by classification uncertainty, sensor differences, and environmental variability. Therefore, the findings should be interpreted as indicative trends rather than exact measurements. This study highlights the potential of integrating remote sensing and machine learning approaches for long-term monitoring of mangrove ecosystems and provides useful information to support mangrove conservation and management strategies.

KEYWORDS: Google Earth Engine; Landsat, Mangrove; Random Forest; MVI; NDVI

INTRODUCTION

Mangrove forests are among the most productive coastal ecosystems, providing critical habitat for a wide range of marine and terrestrial species, protecting shorelines from erosion, and sequestering carbon at rates two to four times higher than those of terrestrial forests (Friess et al., 2019; Pimple et al., 2020; Murdiyarso et al., 2015). Despite their ecological and socio-economic value, mangroves are disappearing globally at an estimated 0.2–0.7% yr^{-1}, driven primarily by land-use conversion, aquaculture expansion, and climate-induced sea-level rise (Ali & Nayyar, 2020; Bryan-Brown et al., 2020; Food and Agricultural Organization of the United Nations, 2020). In Indonesia, rapid coastal development has intensified these pressures, making continuous monitoring essential for effective conservation and management (Gilman, Ellison, Duke, & Field, 2008; Carugati et al, 2018).

Remote sensing has become the cornerstone for large-scale mangrove mapping because traditional field surveys are costly, time-consuming, and often limited by tidal inundation (Goldberg, Lagomasino, Thomas, & Fatoyinbo, 2020). Conventional vegetation indices such as the Normalized Difference Vegetation Index (NDVI) perform well for general vegetation detection but struggle to discriminate mangroves from adjacent terrestrial cover, especially under

varying tidal conditions (Duke et al., 2007; Makowski & Finkl, 2018). Mangrove-specific indices that incorporate short-wave infrared (SWIR) bands—e.g., the Mangrove Vegetation Index (MVI)—have demonstrated superior sensitivity to the unique spectral signature of submerged mangrove canopies (Binh et al., 2022; Peters et al., 2020).

Recent studies in southern Iran have highlighted contrasting trends in mangrove extent, with many sites showing expansion due to rehabilitation efforts, while others continue to decline because of anthropogenic disturbances (Giri et al., 2016; Erfanifard, Lotfi-Nasirabad, & Štěpánek, 2022). However, few investigations have applied the latest cloud-based platforms and machine-learning classifiers to jointly evaluate NDVI and MVI across multiple decades. This study therefore, aims to assess the temporal dynamics of mangrove cover in the Kuala Lupak Nature Reserve from 1990 to 2020 using Landsat imagery, compare the classification accuracy of NDVI- and MVI-derived maps generated with a Random Forest algorithm in Google Earth Engine, and identify spatial patterns of loss and gain to inform targeted conservation actions.

METHODOLOGY

Research Location

The Kuala Lupak Nature Reserve is located in the coastal region of South Kalimantan, directly bordering the Java Sea to the east. Geographically, it is located between 3°26'30"–3°29'55" South Latitude and 114°22'30"–114°29'20" East Longitude. Located southwest of the city of Banjarmasin, Kuala Lupak Nature Reserve is part of an important coastal ecosystem complex on the island of Kalimantan. Maps shown in Figure 1.

Image Data and Pre-Processing

The main data consists of Landsat 5 TM, Landsat 7 ETM+, and Landsat 8 OLI images accessed through the Google Earth Engine (GEE) platform. All images were selected during the peak dry season to minimize cloud interference, in accordance with the recommendations of the latest mangrove mapping studies (Binh et al., 2022; Jiang et al., 2021; Baloloy, Blanco, Ana, & Nadaoka, 2020).

Figure 1. Map of the Kuala Lupak Nature Reserve Research Location

The pre-processing stage includes:

1. Cloud and cloud shadow masking using GEE's built-in pixel_qa algorithm (Fmask-based), which has been proven effective for Landsat images (Zhu & Woodcock, 2015).
2. Automatic radiometric correction by GEE and equalization of reflectance values between sensors.
3. Creation of an annual median composite, as is commonly used for long-term change mapping (Giri, 2016).
4. Clip the study area based on the boundaries of the Kuala Lupak Nature Reserve polygon.

This cloud-based pre-processing provides consistency between years and reduces bias due to atmospheric variability. To ensure consistency across different Landsat sensors (Landsat 5 TM, Landsat 7 ETM+, and Landsat 8 OLI), this study utilized surface reflectance products available in Google Earth Engine, which have been atmospherically corrected using standardized processing algorithms. Although no additional empirical harmonization (e.g., sensor-specific regression coefficients) was applied, consistency was maintained by using equivalent spectral bands (Red, NIR, and SWIR) across sensors and by generating annual median composites. This approach reduces inter-sensor variability and minimizes the influence of short-term environmental noise, although residual differences between sensors may still exist.

Vegetation Index Calculation

Vegetation indices were calculated to improve the model's ability to distinguish between mangroves and non-mangroves. Two indices were used because they have proven effective in mangrove studies over the past decade.

(1) NDVI — Normalized Difference Vegetation Index (NDVI)

NDVI is used as a general indicator of vegetation greenness. Although relatively sensitive to wet substrate conditions in coastal areas, this index remains important as a basic comparison in land cover modeling (Binh et al., 2022; Wang et al., 2020). The formula is:

$$NDVI = \frac{(NIR - Red)}{(NIR + Red)} \quad (1)$$

(2) MVI — Mangrove Vegetation Index (MVI)

MVI is used as the primary index because it is specifically designed for mangroves and performs better in distinguishing mangroves from other coastal vegetation, especially in intertidal areas with strong tidal influences (Baloloy, Blanco, Ana, & Nadaoka, 2020; Xia et al., 2020). The formula is:

$$MVI = \frac{(NIR - Green)}{(SWIR1 - Green)} \quad (2)$$

Both indices are automatically calculated in Google Earth Engine after image pre-processing and are used as additional input variables in Random Forest classification.

Training and Validation Data Design

Training and validation samples were generated through visual interpretation of high-resolution imagery from Google Earth for each observation year (1990, 2000, 2010, and 2020). Two classes were defined: mangrove and non-mangrove.

A stratified random sampling approach was applied to ensure balanced representation of each class. For each year, a total of 25-30 sample points were collected and proportionally distributed across the two classes. The dataset was divided into 70% training data and 30% validation data. To reduce spatial autocorrelation and avoid overestimation of classification accuracy, a minimum distance of approximately 30–50 meters was maintained between training and validation samples. This sampling design ensures independence between datasets and improves the robustness of the classification model.

Random Forest Classification

Mangrove cover classification was performed using the Random Forest (RF) algorithm, which is widely used in remote sensing applications due to its ability to handle multiband data and non-linear relationships (Belgiu & Drăguț, 2016; Maxwell et al., 2018). The input variables used in the classification included spectral bands (Red, Near-Infrared (NIR), and Shortwave Infrared (SWIR)) and two vegetation indices, namely NDVI and Mangrove Vegetation Index (MVI).

These variables were used to develop classification models for each observation year (1990, 2000, 2010, and 2020).

The RF model was implemented in Google Earth Engine with a specified number of trees (nTrees), while other parameters were maintained at default settings to ensure model stability. The trained model was then applied to the corresponding images for each year to generate mangrove distribution maps. In addition to the training-validation scheme described in the previous section, the RF algorithm provides an internal accuracy estimate through the Out-of-Bag (OOB) error, which was used as an additional indicator of model performance.

RF was selected due to its robustness against overfitting and its ability to produce consistent classification results across multitemporal datasets (Pelletier et al., 2019). However, the classification results remain dependent on the quality of input variables and should be interpreted with consideration of potential uncertainty.

Accuracy Test

Accuracy assessment was conducted using an independent validation dataset. The evaluation included Overall Accuracy (OA), Kappa Coefficient, Producer's Accuracy (PA), and User's Accuracy (UA), all derived from confusion matrices. The confusion matrix provides detailed information on classification performance for each class and allows identification of omission and commission errors. It should be noted that very high accuracy values (e.g., OA = 1.00 and Kappa = 1.00) are uncommon in real-world classification and may be influenced by sample size, class separability, and spatial distribution of validation data. Therefore, the results are interpreted with caution, and potential sources of bias are acknowledged.

Mangrove Change Analysis

Changes were analyzed using a post-classification comparison approach, which compares classification results between years to obtain change classes: gain (mangrove addition); loss (mangrove loss); stable mangrove (permanent mangrove); and stable non-mangrove. This approach is widely used in long-term mangrove dynamics mapping studies because it is more accurate than single index-based methods (Erfanifard, Khodakarami, & Cheraghi, 2022; Fatoyinbo, Lagomasino, Feliciano, & Lee, 2018).

The post-classification comparison approach inherently accumulates classification errors from each time period. Therefore, uncertainties from individual classification results may propagate into the change detection outcomes. This limitation is considered in the interpretation of mangrove gain and loss, and the results should be viewed as indicative rather than absolute values.

Limitations and Uncertainty

Several limitations should be considered in this study. First, despite the use of surface reflectance products, residual differences between Landsat sensors may still influence spectral consistency. Second, tidal variability may affect mangrove spectral responses, even though image selection and compositing were designed to minimize this effect. Third, the sampling design and limited validation data may introduce bias in the accuracy assessment. Finally, uncertainties from classification results may propagate into change detection analysis. These limitations highlight the need for cautious interpretation and suggest opportunities for future improvement through the integration of additional datasets and more advanced validation techniques.

RESULTS AND DISCUSSION

NDVI and MVI Distribution Patterns

The results of NDVI and MVI calculations show variations in vegetation conditions across the observation years. NDVI represents general vegetation greenness, while MVI provides improved contrast for mangrove identification due to its sensitivity to moisture and canopy structure through the Shortwave Infrared (SWIR) band.

The spatial distribution of the NDVI and MVI is shown in Figures 2 and 3 values indicate that areas with high index values correspond to dense and healthy mangrove

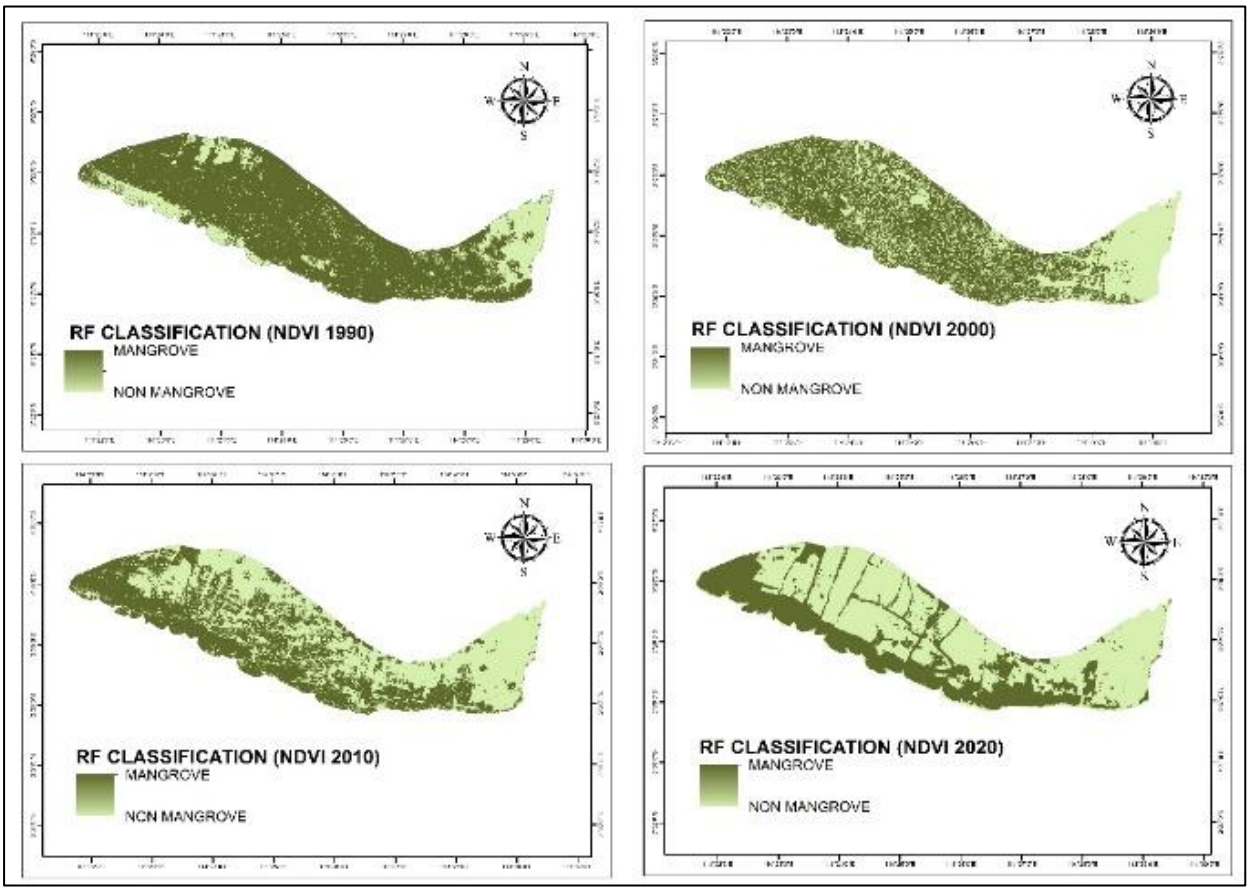

Figure 4. NDVI Classification Results – Random Forest

vegetation, whereas low values represent sparse vegetation, open land, or inundated areas. In general, MVI appears to provide clearer delineation of intertidal mangrove zones compared to NDVI. However, this visual distinction should be interpreted cautiously, as spectral responses in coastal environments are influenced by tidal conditions, soil moisture, and atmospheric variability. Therefore, differences observed between NDVI and MVI are not solely attributed to index performance but may also reflect environmental conditions during image acquisition.

Random Forest Classification Results

Mangrove classification using the Random Forest algorithm resulted in two main classes: mangrove and non-mangrove. The classification maps for each observation year (1990, 2000, 2010, and 2020) show noticeable spatial variations in mangrove distribution. The classification results derived from the NDVI and MVI are shown in Figure 4 and Figure 5 indicate a general trend of mangrove decline over time. Spatially, reductions in mangrove cover are more prominent in the eastern and southern parts of the study area, while relatively stable mangrove zones are still observed in the northeastern region. To support the spatial interpretation, the extent of mangrove and non-mangrove areas for each year is presented in the following Table 1.

Table 1. Mangrove and Non-Mangrove Areas Based on NDVI and MVI

Year	Mangrove Area (Ha)	
	NDVI	**MVI**
1990	2578.720007	2659.784086
2000	1898.709031	2392.235929
2010	1,600.818847	1,570.851436
2020	1258.728074	1118.700239
Year	**Non-Mangrove Area (Ha)**	
	NDVI	**MVI**
1990	713.0502021	630.7119653
2000	1393.061179	899.5342805
2010	1690.951362	1716.455448

Table 1 confirms that mangrove area has decreased consistently over the study period, while non-mangrove areas have increased correspondingly. Differences between NDVI

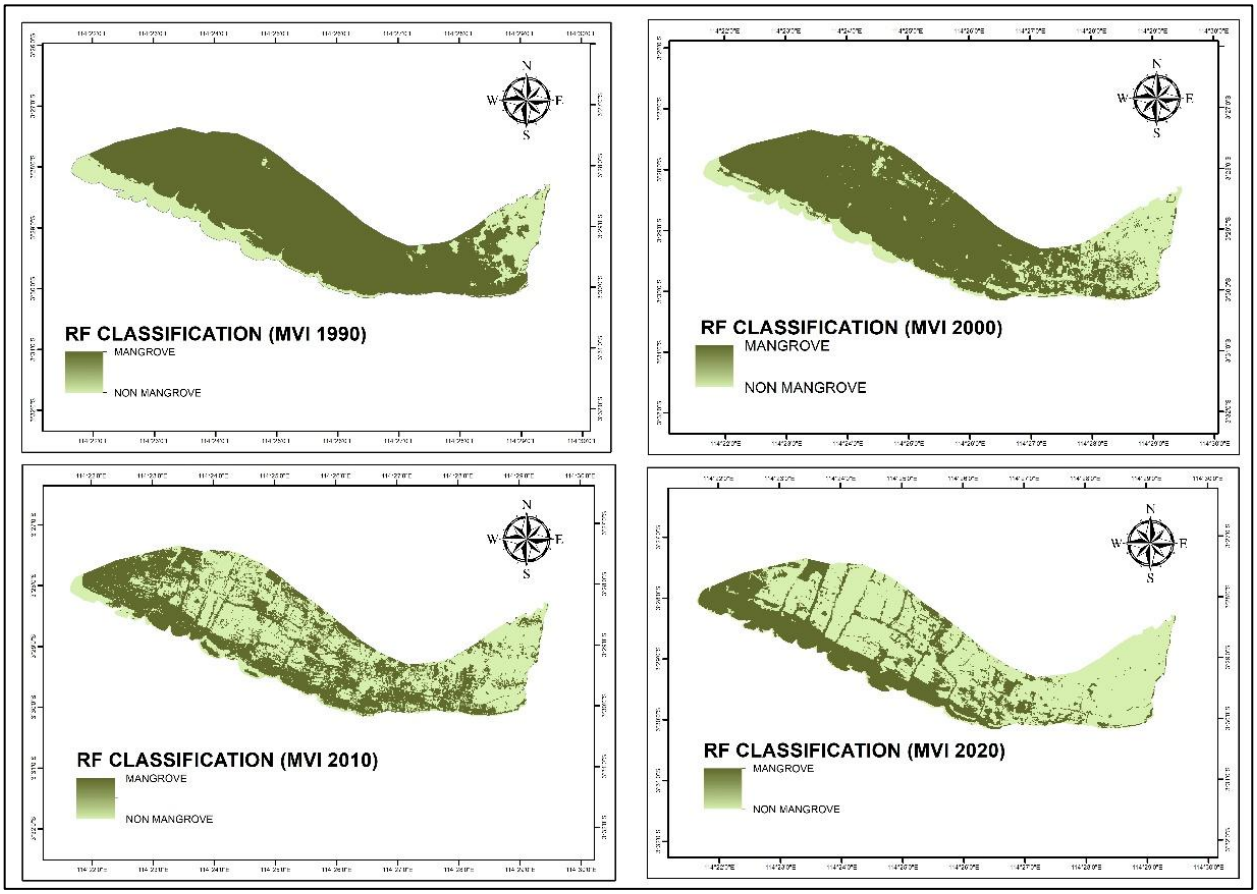

Figure 5. MVI Classification Results – Random Forest

and MVI estimates are also observed, reflecting variations in index sensitivity to mangrove characteristics, particularly in coastal and intertidal environments. It is important to note that classification results are influenced by the quality and spatial distribution of training samples. Although Random Forest is robust against overfitting, classification outputs still represent the best approximation based on available data rather than exact ground conditions. Therefore, interpretation of spatial patterns should consider potential classification uncertainty, especially in transitional areas between mangrove and non-mangrove classes.

Accuracy Test

Accuracy testing was performed using Overall Accuracy (OA) and Kappa Coefficient generated directly from the Random Forest classification process on Google Earth Engine. The accuracy values for the NDVI and MVI methods are shown in Table 2 and Table 3. The accuracy assessment results indicate that both NDVI- and MVI-based classifications achieved generally high performance across all observation years. MVI shows more consistent accuracy values, while NDVI exhibits greater variability between years. In some cases, very high accuracy values were obtained (OA = 1.00 and Kappa = 1.00). While these results suggest strong class separability, such perfect accuracy is uncommon in real-world remote sensing applications. These values may be influenced by factors such as sample size, class homogeneity, or spatial proximity between training and validation data. Therefore, the results should be interpreted with caution. The inclusion of producers' and users' accuracy, along with confusion matrices, provides a more detailed understanding of classification performance and helps identify potential sources of misclassification.

Table 2. Overall Accuracy and Kappa Coefficient of NDVI classification

Year	Overall Accuracy	Kappa	Description
1990	0.9375	0.875	Excellent
2000	0.733	0.4736	Good
2010	0.95	0.899	Excellent
2020	1	1	Excellent

Table 3. Overall Accuracy and Kappa Coefficient of MVI classification

Year	Overall Accuracy	Kappa	Description
1990	1	1	Excellent
2000	0.9	0.7647	Very Good
2010	0.9375	0.875	Excellent
2020	1	1	Excellent

Spatial Changes in Mangroves (1990–2020)

The analysis of mangrove cover change during the period 1990–2020 reveals a dominant trend of mangrove loss across the study area. Based on the post-classification comparison approach, four change categories were identified, namely gain, loss, stable mangrove, and stable non-mangrove. The quantitative results of these changes are presented in Table 4.

As shown in Table 4, the total area of mangrove loss (1,857.15 ha) is substantially higher than the gain area (318.15 ha), resulting in an estimated net loss of approximately 1,539 ha over the 30-year period. This indicates that mangrove degradation has occurred more extensively than regeneration within the study area. However, it is important to note that these values are derived from a post-classification comparison approach, which may accumulate classification errors from each time period. Therefore, the reported change values should be interpreted as indicative estimates rather than exact measurements.

Table 4. Area of mangrove change from 1990 to 2020

Category	Area (Ha)	Description
Gain	318,149	Non-mangrove area in 1990 that turned into mangrove in 2020
Loss	1,857.15	The mangrove area in 1990 that was lost in 2020
Stable Mangrove	311.67	The area that remained mangrove in both periods
Stable Non-Mangrove	809,549	Permanent non-mangrove area without forest cover

The spatial distribution of mangrove dynamics is illustrated in Figure 6, which shows a clear directional pattern of change. As observed in Figure 6, areas of mangrove loss are predominantly located in the eastern and southern parts of the study area, while gain areas are more limited and tend to occur in the western coastal region. Stable mangrove areas

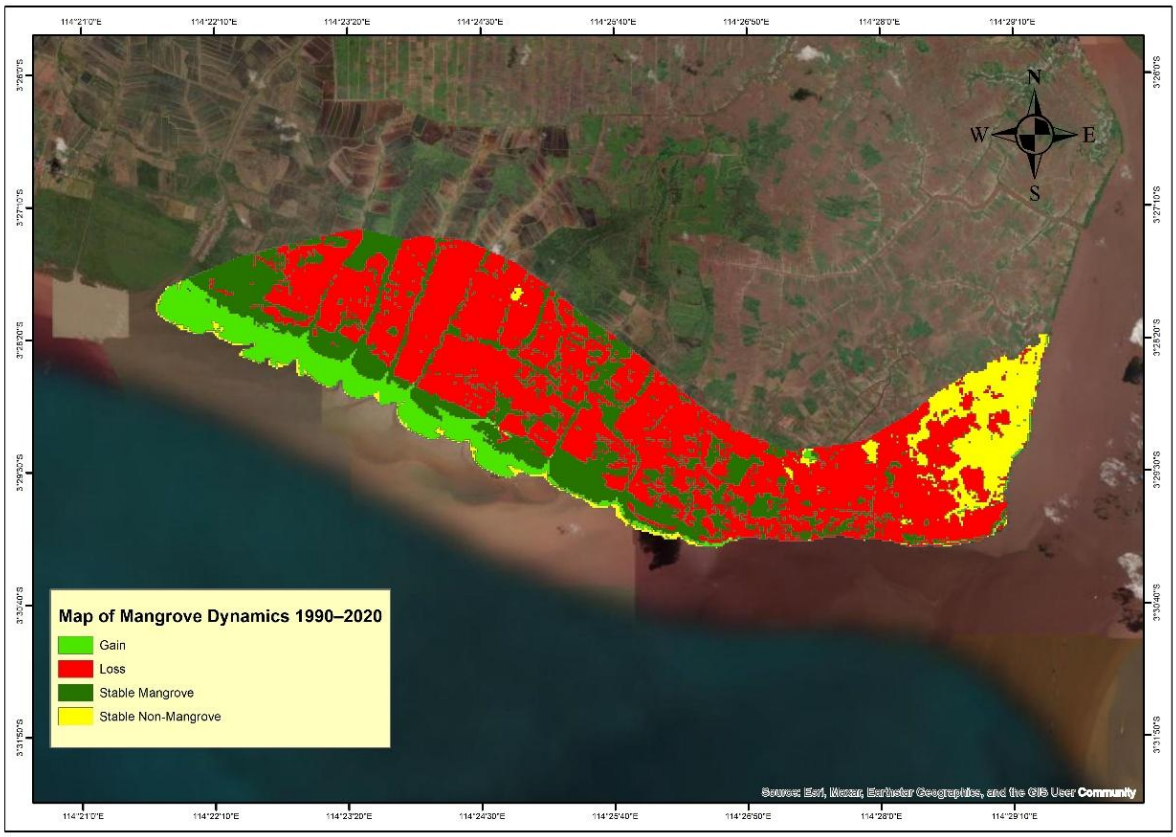

Figure 6. Map of Mangrove Dynamics 1990–2020

are mainly found in relatively protected zones, whereas stable non-mangrove areas dominate inland regions that have not experienced significant changes. Although this spatial pattern is clearly visible, it should be interpreted with caution, particularly in transitional zones where class boundaries may be less distinct and more susceptible to classification uncertainty.

The observed pattern of mangrove loss may be associated with anthropogenic activities and coastal environmental dynamics, such as land-use conversion, aquaculture expansion, and changes in hydrodynamic conditions. However, this study does not incorporate independent spatial datasets—such as land-use maps, shoreline change data, or sedimentation data—to directly validate these drivers. Therefore, the interpretation of causal factors remains inferential and should be considered as a potential explanation rather than a definitive conclusion.

Despite these limitations, the overall trend indicates a consistent decline in mangrove extent over the study period. This finding is in line with observations from other tropical coastal regions, where mangrove degradation often exceeds natural regeneration rates.

Analysis of Mangrove Dynamics 1990–2020 and Comparison with Previous Studies

The dynamics of mangrove change during the 1990–2020 period show a combination of areas experiencing increase and decrease, with a more dominant downward trend. A pixel-by-pixel comparison between 1990 and 2020 reveals a consistent spatial pattern: areas of loss are concentrated in the east to south, while areas of gain appear in more limited areas and are more prevalent in the west and at several points near the estuary. The fairly large area of stable mangroves shows that some areas have maintained stable ecological conditions, despite ongoing environmental pressures.

This spatial pattern is consistent with the temporal dynamics observed in the mangrove area time series. Visualization through a bar chart in Figure 7. Diagram of Mangrove Area Change 1990–2020 shows a gradual and continuous decline over three decades, suggesting a general trend of mangrove degradation over time. The presence of gain areas indicates that regeneration is still occurring; however, it appears insufficient to offset the more extensive loss observed in the study area.

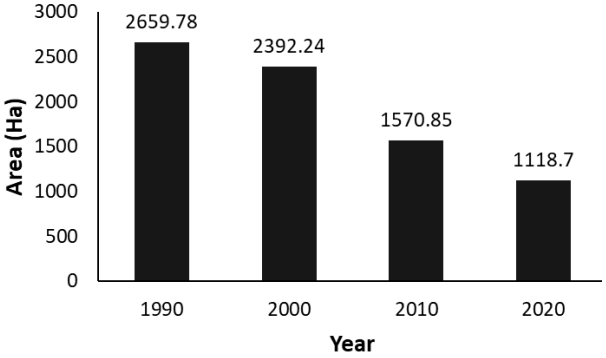

Figure 7. Diagram of Mangrove Area Change 1990–2020

It should be noted that these patterns are derived from classified satellite data and may be influenced by classification uncertainty, environmental variability, and sensor differences. Therefore, the results should be interpreted as indicative trends rather than exact representations of change.

A comparison with the study by Erfanifard et al. (2022) on the coast of Iran reveals similar long-term dynamics, characterized by the coexistence of mangrove expansion and degradation driven by a combination of natural processes and human activities. Both regions demonstrate that areas with relatively stable geomorphological conditions tend to maintain mangrove cover, whereas areas undergoing environmental changes exhibit higher levels of loss.

However, this study does not incorporate independent spatial datasets (e.g., land-use change, shoreline dynamics, or sedimentation data) to directly assess the drivers of change. Therefore, any interpretation of causal factors remains inferential and should be considered as a potential explanation rather than a definitive conclusion. In this context, the comparison between NDVI and MVI is primarily based on their performance within the Random Forest classification framework. A more rigorous evaluation of their relative performance would require additional statistical testing, which is beyond the scope of this study.

CONCLUSION

This study demonstrates that the integration of multitemporal Landsat imagery with vegetation indices (NDVI and MVI) and Random Forest classification can be used to analyze mangrove dynamics in the Kuala Lupak Nature Reserve. The results indicate that MVI generally provides more stable classification performance compared to NDVI, particularly in distinguishing mangrove and non-mangrove areas in coastal environments.

The analysis of mangrove change from 1990 to 2020 reveals a general trend of decreasing mangrove extent, with loss areas exceeding gain areas over the study period. Spatial patterns show that mangrove decline is more prominent in certain parts of the study area, while limited regeneration occurs in other areas. However, it is important to note that the results are derived from classified satellite imagery and may be influenced by classification uncertainty, sensor differences, and environmental variability. In addition, this study does not incorporate independent spatial datasets to directly assess the drivers of mangrove change. Therefore, interpretations regarding causal factors should be considered as indicative rather than definitive.

Overall, this study highlights the importance of remote sensing-based monitoring for understanding long-term mangrove dynamics. Future research is recommended to integrate additional spatial datasets and more advanced validation approaches to improve the reliability of change detection and to better support mangrove management and conservation efforts.

ACKNOWLEDGEMENT

The authors are grateful to the Ministry of Education, Culture, Study, and Technology for funding this study through the National Postgarduate Research Grant [Number 1462/UN8.2/PG/2025]. This support was instrumental in conducting and completing this study.

REFERENCES

Ali, A., & Nayyar, Z. A. (2020). Extraction of mangrove forest through Landsat-8 mangrove index (L8MI). *Arabian Journal of Geosciences*, 13, 1–12.

Baloloy, A. B., Blanco, A. C., Ana, R. R. C. S., & Nadaoka, K. (2020). Development and application of a new mangrove vegetation index (MVI) for rapid and accurate mangrove mapping. *ISPRS Journal of Photogrammetry and Remote Sensing*, 166(1), 95–117.

Belgiu, M., & Drăguț, L. (2016). Random forest in remote sensing: A review of applications and future directions. *ISPRS Journal of Photogrammetry and Remote Sensing*, 114, 24–31.

Binh, N., Hauser, L., Hoa, P., Thao, G., An, N., Nhut, H., Phuong, T., & Verrelst, J. (2022). Quantifying mangrove leaf area index from Sentinel-2 imagery using hybrid models and active learning. *International Journal of Remote Sensing*, 43, 1–15.

Bryan-Brown, D. N., Connolly, R. M., Richards, D. R., Adame, F., Friess, D. A., & Brown, C. J. (2020). Global trends in mangrove forest fragmentation. *Scientific Reports*, 10, 7177.

Carugati, L., Gatto, B., Rastelli, E., Martire, M. L., Coral, C., Greco, S., & Danovaro, R. (2018). Impact of mangrove forest degradation on biodiversity and ecosystem functioning. *Scientific Reports*, 8, 13298.

Duke, N. C., Meynecke, J.-O., Dittmann, S., Ellison, A. M., Anger, K., Berger, U., Cannicci, S., et al. (2007). A world without mangroves? *Science*, 317, 41–42.

Erfanifard, Y., Khodakarami, L., & Cheraghi, S. (2022). Long-term dynamics of mangroves in the Persian Gulf using Landsat imagery (1990–2020). *Estuarine, Coastal and Shelf Science*, 268, 107741.

Erfanifard, Y., Lotfi-Nasirabad, M., & Štěpánek, K. (2022). Assessment of Iran's mangrove forest dynamics (1990–2020) using Landsat time series. *Remote Sensing*, 14, 4912. https://doi.org/10.3390/rs14194912

Fatoyinbo, T. E., Lagomasino, D., Feliciano, E., & Lee, S. (2018). Mangrove extent changes and drivers across global deltas.

Environmental Research Letters, 13(5), 054008.

Food and Agriculture Organization of the United Nations. (2020). Global forest resources assessment 2020: *Main report*. FAO.

Friess, D. A., Rogers, K., Lovelock, C. E., Krauss, K. W., Hamilton, S. E., Lee, S. Y., Lucas, R., Primavera, J., Rajkaran, A., & Shi, S. (2019). The state of the world's mangrove forests: Past, present, and future. *Annual Review of Environment and Resources*, 44, 89–115. https://doi.org/10.1146/annurev-environ-101718-033302

Gilman, E. L., Ellison, J., Duke, N. C., & Field, C. (2008). Threats to mangroves from climate change and adaptation options: A review. *Aquatic Botany*, 89, 237–250. https://doi.org/10.1016/j.aquabot.2007.12.009

Giri, C. (2016). Observation and monitoring of mangrove forests using remote sensing: Opportunities and challenges. *Remote Sensing*, 8(9), 783. https://doi.org/10.3390/rs8090783

Giri, C., Ochieng, E., Tieszen, L. L., Zhu, Z., Singh, A., Loveland, T., et al. (2016). The global distribution and extent of mangrove forests: A review of current knowledge. *Remote Sensing*, 8, 783.

Goldberg, L., Lagomasino, D., Thomas, N., & Fatoyinbo, T. (2020). Global declines in human-driven mangrove loss. *Global Change Biology*, 26, 5844–5855. https://doi.org/10.1111/gcb.15275

Jiang, Y., Zhang, L., Yan, M., Qi, J., Fu, T., Fan, S., & Chen, B. (2021). High-resolution mangrove forest classification with machine learning using WorldView and UAV hyperspectral data. *Remote Sensing*, 13(8), 1529. https://doi.org/10.3390/rs13081529

Makowski, C., & Finkl, C. (2018). *Threats to mangrove forests*. Springer.

Maxwell, A. E., Warner, T. A., & Fang, F. (2018). Implementation of machine-learning classification in remote sensing: An applied review. *International Journal of Remote Sensing*, 39(9), 2784–2817. https://doi.org/10.1080/01431161.2018.1433343

Millard, K., & Richardson, M. (2015). On the importance of training data sample selection in random forest image classification: A case study in peatland ecosystem mapping. *Remote Sensing*, 7(7), 8489–8515. https://doi.org/10.3390/rs70708489

Murdiyarso, D., Purbopuspito, J., Kauffman, J. B., Donato, D., Warren, M. W., Sasmito, S. D., Manuri, S., et al. (2015). The potential of Indonesian mangrove forests for global climate change mitigation. *Nature Climate Change*, 5, 1089–1092. https://doi.org/10.1038/nclimate2734

Pelletier, C., Webb, G. I., & Petitjean, F. (2019). Temporal convolutional neural network for the classification of satellite image time series. *Remote Sensing*, 11(5), 523. https://doi.org/10.3390/rs11050523

Peters, R., Walther, M., Lovelock, C., Jiang, J., & Berger, U. (2020). The interplay between vegetation and water in mangroves: New perspectives for mangrove stand modeling and ecological research. *Wetland Ecology and Management*, 28, 697–712.

Pimple, U., Simonetti, D., Hinks, I., Oszwald, J., Berger, U., Pungkul, S., et al. (2020). A history of the rehabilitation of mangroves and an assessment of their diversity and structure using Landsat annual composites (1987–2019) and transect plot inventories. *Forest Ecology and Management*, 462, 118007.

Thomas, N., Lucas, R., Bunting, P., Hardy, A., Rosenqvist, A., & Fatoyinbo, T. (2019). Mapping mangrove extent and change using global-scale remote sensing. *Remote Sensing of Environment*, 233, 111.

Wang, L., Duan, Y., Zhang, L., Rehman, T. U., Ma, D., & Jin, J. (2020). Precise estimation of NDVI with a NIR-sensitive RGB camera and machine learning methods for corn plants. *Sensors*, 20(12), 3208.

Xia, Q., Qin, C.-Z., Li, H., Huang, C., Su, F.-Z., & Jia, M.-M. (2020). Evaluation of submerged mangrove recognition index

using multi-tidal remote sensing data. *Ecological Indicators*, 113(1), 106196. https://doi.org/10.1016/j.ecolind.2020.106196

Zhu, Z., & Woodcock, C. E. (2015). Automated cloud and cloud-shadow detection in Landsat imagery. *Remote Sensing of Environment*, 152, 217–234.